Robotic injection of zebrafish embryos for high-throughput screening in disease models ☆

Herman P. Spaink [a,*], Chao Cui [b], Malgorzata I. Wiweger [a,b], Hans J. Jansen [b], Wouter J. Veneman [a], Rubén Marín-Juez [b], Jan de Sonneville [c], Anita Ordas [a], Vincenzo Torraca [a], Wietske van der Ent [a], William P. Leenders [d], Annemarie H. Meijer [a], B. Ewa Snaar-Jagalska [a], Ron P. Dirks [b]

[a] Department of Molecular Cell Biology, Institute of Biology, Leiden University, The Netherlands
[b] ZF-screens B.V., Leiden, The Netherlands
[c] Life Science Methods B.V., Leiden, The Netherlands
[d] Department of Pathology, Radboud University Nijmegen Medical Centre, Nijmegen, The Netherlands

ARTICLE INFO

ABSTRACT

The increasing use of zebrafish larvae for biomedical research applications is resulting in versatile models for a variety of human diseases. These models exploit the optical transparency of zebrafish larvae and the availability of a large genetic tool box. Here we present detailed protocols for the robotic injection of zebrafish embryos at very high accuracy with a speed of up to 2000 embryos per hour. These protocols are benchmarked for several applications: (1) the injection of DNA for obtaining transgenic animals, (2) the injection of antisense morpholinos that can be used for gene knock-down, (3) the injection of microbes for studying infectious disease, and (4) the injection of human cancer cells as a model for tumor progression. We show examples of how the injected embryos can be screened at high-throughput level using fluorescence analysis. Our methods open up new avenues for the use of zebrafish larvae for large compound screens in the search for new medicines.

© 2013 The Authors. Published by Elsevier Inc. All rights reserved.

1. Introduction

The use of zebrafish as an animal model has an abundance of applications in fundamental research in vertebrate development, physiology and toxicology [4,11,37,78,79]. More recently, this model has also been shown to be highly applicable for studies of many types of disease [1,2,5,9,35,44,52,55,57,59–61,73–75]. The benefits of the relatively small and transparent larvae for optical imaging using transgenic fish lines expressing many colour varieties of the GFP protein have been widely exploited in these disease studies [1]. Currently the genetic tool box is comprised of a large variety of gene knock-down or knock-out systems [6,10,14,20,21,25,43,64]. Additionally many genomic-based techniques such as RNA deep sequencing, metabolomics and proteomics have been applied to zebrafish [17–19,40,42,45,53,54, 66,71,97]. A comparison of parallel deep RNA sequencing and proteome analysis has been reported (Palmblad et al., submitted).

The fact that the innate immune system of zebrafish is highly similar to that of mammals and is already fully functional as early as two days after fertilization makes zebrafish larvae extremely useful for studies of diseases related to the immune system [72,94]. Examples given below are studies of cancer progression and infectious diseases caused by many bacteria, fungi or viruses.

1.1. Zebrafish microinjection and screening tools

Microinjection of zebrafish embryos is an essential technology for the following applications:

- The generation of transgenic zebrafish lines.
- The generation of gene knock-out lines using zinc fingers or TALEN technology.
- Gene knock-down using morpholinos, siRNA or antibodies.
- Overexpression of genes by injection of mRNA.
- The injection of tracer dyes or particles.
- Intraorganismal introduction of microbes in embryos or larvae for infection studies.
- Transplantation of cells between embryos.
- Xenograft implantation of cells for cancer studies.

---

* Corresponding author. Address: Einsteinweg 55, 2333 CC Leiden, The Netherlands.

E-mail address: h.p.spaink@biology.leidenuniv.nl (H.P. Spaink).

Many general methods for these applications can be found in the book: Essential Zebrafish Methods: Cell and Developmental Biology [26]. More specifically for injection methods that can be used for these applications we can refer to detailed descriptions in four methodology compendia or books: (1) Zebrafish: Methods and Protocols [51], (2) The zebrafish book, A guide for the laboratory use of zebrafish (*Danio rerio*), 5th edition [99] and (3) Methods in Cell Biology issues 104 and 105 [27,28], which provide comprehensive laboratory protocols and reviews for recent zebrafish methods related to disease models and chemical screens. Recently also video enhanced protocols for zebrafish microinjection have been published, for instance by Benard et al. [7], describing in detail the application of microinjection of bacterial pathogens. In brief, all methods use thin glass capillary needles to introduce compounds or biological materials inside various parts of embryos and larvae. In the embryonic and early larval stages the transparency and softness of the tissues warrants a high success rate of the injection protocol. In contrast, injection in the later larval stages is more difficult due to higher rigidity of tissue and can currently only be performed at relatively low throughput. For the first four applications mentioned above, DNA, RNA or morpholinos can be injected into the yolk of early stage embryos. Due to the relatively large size of the yolk this offers a fast procedure for microinjection that even can be completely automated. Robotic injection of zebrafish embryos using image recognition has been shown to accurately deliver morpholinos at a throughput level of 25 consecutive injections per run of 2 min [98]. Recently an alternative robotic injection method was shown to inject embryos at a speed of 2000 per hour with a success rate of 99% [15]. This method makes use of specially designed grids where embryos occupy the hemi-spherical wells of an agarose cast in a centred and completely reproducible manner, with the cell mass always resting to the side. In this paper we present further applications and detailed methods for the use of this robotic injection system. We will also provide examples of high-throughput screening of injected embryos. Screening of zebrafish embryos can make use of the rapid technical advances in high-throughput analysis methods for zebrafish embryos [1,33,47]. The COPAS XL (Complex Object Parametric Analyzer and Sorter) system (Union Biometrica) can be used for fluorescence imaging of zebrafish embryos at a throughput level of 200 embryos per minute. This system has been designed for the analysis, sorting and dispensing of objects up to 1.5 mm in diameter based on size, optical density and fluorescence intensity. A profiler option simultaneously detects and analyzes up to 8000 data points per object for each of the channels of extinction and fluorescence, and includes advanced imaging options. The resulting profiles can be used to set parameters for zebrafish larvae to be sorted in 96-wells plates. In this paper we describe software to process the recorded data for further statistical analysis. Recently a vertebrate automated screening technology (VAST) with cellular-resolution and parallel animal processing has been reported in which the screening throughput is limited only by the image acquisition speed rather than by the fluidic or mechanical processes [16,67]. In the near future we will also use this methodology for zebrafish high content image analysis aimed at disease screening at high-throughput such as discussed below.

1.2. Applications of microinjection for studies of infectious disease

A growing list of pathogenic bacteria, filamentous fungi, yeasts, microsporidia, helminths, trypanosomes and viruses has been used for experimental infection studies in zebrafish, as detailed in several recent reviews [12,23,24,46,57,58,65,73]. Bacterial pathogens have been tested most frequently, as discussed by Meijer and Spaink [57] who present an overview of over 30 bacterial species for which disease studies in zebrafish have been published. In addition, zebrafish larvae have also been used to study the effects of a bacterial strains that normally do not cause a disease, *Staphylococcus epidermidis*, for the purpose of studying the effects of factors such as medical implant materials on defence mechanisms against commensal bacteria [97]. One of the most successful zebrafish disease models is the indirect study of human tuberculosis via the infection of zebrafish embryos with *Mycobacterium marinum*, as recently reviewed by Tobin, May and Wheeler [91]. The studies of *M. marinum* infection have already led to the clarification of many important processes in the life cycle of tuberculosis infection, in particular those underlying the mechanisms of granuloma formation in which the bacteria proliferate in macrophages [8,92]. The context of the embryo's developing immune system makes it possible to study the contribution of different immune cell types to disease progression already at 1–2 days post fertilization, when functional macrophages and neutrophil develop. Furthermore, due to the clear temporal separation of innate immunity from adaptive responses, zebrafish larvae are particularly useful for dissecting the innate host factors involved in pathology. Recent studies have underscored the remarkable similarity of the zebrafish and human immune systems, which is important for biomedical applications [94]. Since conserved pathogen associated molecular pattern recognition systems are already functional at one day post fertilization, zebrafish embryos and larvae are highly suitable for rapid screening of disease progression up to the stage that feeding becomes necessary and ethical constraints become apparent [85]. For infection studies a common route of infecting zebrafish embryos is the injection of the pathogen into the caudal vein of 1 day old embryos [7]. This method is relatively labour-intensive and although it has been successfully used for drug screens [86] it compares to cellular screening technologies as a low throughput technique, leading to major bottlenecks in drug discovery. Since infection by immersion in most infection models is not an effective alternative [96], we sought to achieve a reliable high-throughput automatic injection system, drastically reducing the man-hour requirement while vastly increasing the number of reproducibly infected embryos. As shown by Carvalho et al. [15] and Veneman et al. [97] we have successfully used robotic microinjection technology for screening bacterial proliferation during the first 5 days of larval development. In these studies the COPAS technology mentioned above was used to monitor bacterial proliferation. Carvalho et al. [15] have also shown that this high-throughput injection method, by its versatile applicability in small high safety flow cabinets, can be used for the study of infection by dangerous human pathogens such as *Mycobacterium tuberculosis* owing to the fact that this bacterial species can survive within macrophages of zebrafish larvae.

1.3. Applications of microinjection for studies of cancer progression

The zebrafish is increasingly used as a model for the study of cancer progression and metastatic potential of tumor cells [3,31,48,59,68,100]. The optical transparency of zebrafish larvae has permitted novel insights into mechanisms underlying tumor cell migration and the role of host recognition factors that are highly useful for the study of human cancers [32,32,39,90]. High-throughput methodologies have been applied in oncologic small molecules screens in zebrafish [80,88,89,93], however, testing has mainly been performed by addition of potential therapeutic drugs to the swimming water of zebrafish as microinjection of drugs has been hampered by technical limitations in the throughput level. However, the use of artificial carriers that can be used for slow release of drugs has been shown to be highly applicable for future screening for efficacy or toxicity of therapeutics in zebrafish [69]. Especially promising for disease studies in general is the use of photodegradable biogels that can be used for controlled release

of compounds [70]. Microinjection technology has been extensively applied for xenografting of cancer cells and non-transformed cells, including stem cells [22,29,38,39,48,50,63,83,87]. It was shown that many cancer cell types from mammalian origin can survive for extended periods during larval development and that proliferation and spreading can be monitored using automated methods [34]. Clonal zebrafish lines which allow serial transplantations of tumor cells from one fish to another without detrimental gamma-irradiation or usage of immunosupressants can be used for studying the behaviour of xenografted tumor cells in zebrafish after an adaptive immune system has developed [62]. Various studies have explored the possibilities for injecting cancer cells in different tissues of zebrafish embryos or larvae during different developmental stages. For instance injection of mammalian cancer cells into the yolk, cardinal vein, duct of Cuvier, or hindbrain can lead to efficient proliferation and spreading, depending on which tumor cell line is used [22,29,34,38,39,50,83]. It has been indicated that automatic robotic injection of tumor cells can also be performed using robotic technology [15]. In this paper we provide methods for automated injection of tumor cells in early pre-gastrulation stage zebrafish embryos and we show how this method can be used for screening of cancer cell proliferation and spreading.

2. Methodology

2.1. General injection and screening protocol

Robotic microinjection was performed using needles from the company Qvotek (Table 1). For comparisons we have used borosilicate glass capillary needles [7], made with a Harvard Apparatus needle puller. Although these needles are perfectly suitable for manual injection, the commercial needles were needed for robotic injection in order to obtain highly reproducible results. For DNA, morpholino and bacterial injections, needles with an inner tip diameter of 10 µm were used, whereas for cancer cell injections needles with an inner diameter of 20 µm were used. For injection we used a specially designed grid that has been described previously by Carvalho et al. [15]. Zebrafish embryos were placed on a 1% agarose covered grid with a featured honeycomb pattern consisting of 1024 hemi-spherical wells (1.3 mm diameter), except for DNA injection where a new grid with 9 blocks of 100 wells was used. The embryo grid was placed in a motorized stage coupled to a controller and a motorized micro-manipulator. The loaded injection needle was placed in the Injectman II (Eppendorf). The injection height was set using a new precise z-calibration unit (Life Science Methods BV), consisting of a prism fixed next to a hole in the multi-well plate holder which offers a side-view of the needle (Qvotech) when lowered into this hole. For calibration the hole is centered above the lens and a needle is lowered into the hole until a dot appears on the screen. The user then clicks on the dot to center the needle with a precision of smaller than 4 pixels (10 µm). Subsequently, the prism is centered above the lens and the needle is moved to the focal plane of the prism. On the screen a side view of the needle appears and the user clicks on the tip of the needle to calibrate the needle height with equal precision. This 3D datum position is then used to calculate the injection point in the egg with an accuracy of 10 µm in 3D. All components were connected to the controlling computer (linutop, www.linutop.com), which was equipped with a software control program written in python (Life Science Methods BV). For subsequent high-throughput screening we made use of the COPAS-XL (Union Biometrica) as described previously [15,97]. For post sorting analysis of the data we have developed a new script, written in the software package Perl, which can show the distribution of fluorescence pixels in the body of zebrafish larvae as demonstrated with data shown in the bacterial infection section (Figs. 1 and 2).

2.2. Injection of DNA

We injected a DNA construct containing a GFP fusion gene (beta actin promoter-NLSmCherry-IRES-GFP) in the Gateway Tol2 vector together with Tol2 transposase RNA using standard protocols [51]in the middle of the yolk before the first cell-stage. This resulted in fluorescence outside of the yolk at 6 days post implantation (DPI) in 15% of the cases (results not shown). High-throughput injection in combination with subsequent COPAS sorting of fluorescent larvae could make up for this low yield. However, since it has been reported that DNA-constructs should be injected close to or inside the first cell of the embryo proper to improve integration efficiency, an alternative semi-automated solution was developed. A new macro was developed to move the stage to an egg, show an image of the egg, after which the user determines the best injection spot. The pointer is moved to this spot and a mouse-click initiates an injection. After the injection the macro moves the robot to the next egg. Injections were performed close to the cell and in the first cell, and yield was measured as number of embryos showing fluorescence outside the yolk divided by the total number of injected embryos at 6 DPI using a Leica MZ16FA stereo fluorescence microscope. To reduce the delay between different sets of injections, a new grid was used featuring nine blocks of 100 wells. Using a scalpel the agarose grid was cut after injections and the blocks were harvested separately. The yield of semi-automated DNA injection directed just under the first cell is shown in Table 2 demonstrating a yield (at 6 DPI) that is similar to manual injection when COPAS sorting is used (Table 2), however the throughput (<5 s per egg) as well as simplicity (one mouse click) of semi-automated injection is far greater. The semi-automated injections of DNA will be fully automated for future applications by recording a database of images together with their best injection spot. Automated image recognition can be used to find the best correlating image from this database. As such we expect to achieve a speed of 1500 eggs per hour for DNA constructs. In order to achieve this we still need to optimise the lighting as we currently use ambient light.

2.3. Injection of bacteria and screening for bacterial infection

We previously published the development of an automatic injection system for yolk injection in zebrafish embryos [15]. In brief, at 2 h post-fertilization (hpf) or 4 hpf, zebrafish embryos were placed in the 1024 wells agarose grid and injected within half an hour. The system was successfully applied to *M. marinum* and *M. tuberculosis* injection in zebrafish embryos, which serve as a promising model for anti-tuberculosis drug screening [15]. In addition we have also applied this method for injection of *S. epidermidis* at 2 hpf. The results show that the number of injected bacteria is
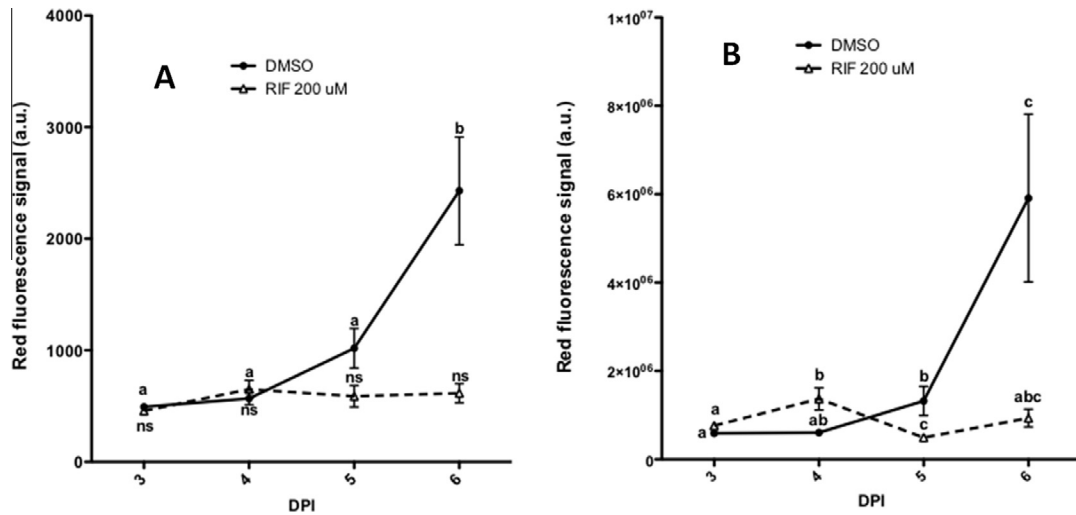
Table 1
Specifications of capillaries (Qvotek, Mississauga, Canada) for robotic intrayolk injection of zebrafish embryos.

Parameter	Value
Start capillary	Borosilicate 100 mm x 1 mm O.D. (0,75 mm I.D.)
Tip end	Beveled and heat-formed spike
Tip angle	No
Orientation of tip opening	Top
Flexibility of tip	Rigid
Taper	Short
Inner tip diameter, bacterial injections	10 µm
Inner tip diameter, tumor cell injections	20 µm

Fig. 1. Progression of the bacterial burden in whole embryos (A) or the tail section of the same embryos (B). Groups of at least 50 embryos were analysed between 3 DPI to 6 DPI and red fluorescent signal was measured and shown in the graphs as mean ± S.E. Different letters indicate statistical significant differences between embryos of the same treatment ($p < 0.05$). ns, no significant differences.
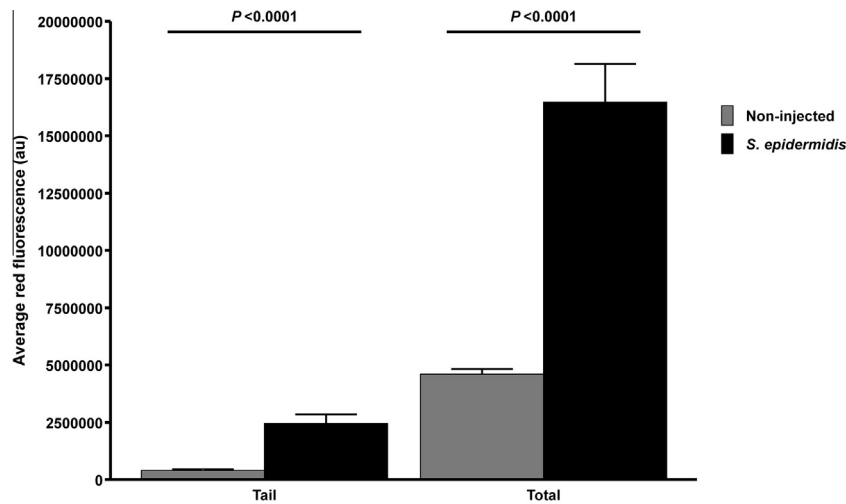

Fig. 2. Quantification of fluorescence intensity of *S. epidermidis* injected embryos using the COPAS XL and PERL macro. The bar graph represents the average fluorescence intensity from 4 biological replica's (70 embryos per group) in the tail and the entire body at 5 DPI (error bars represent SEM).

Table 2

Comparison of different DNA injection methods. Fully-automated and semi-automated methods show 2–3 times higher success rate per minute compared to manual methods (last column). COPAS sorting at 1 DPI can almost double (79% vs 43%) the chance of DNA expression at 6 DPI.

Method	Total inj.	% DNA-expressing embryos at 1 DPI	% DNA-expressing embryos at 6DPI	Inj. time (min)	# inj./min	Successful inj./min
Manual injection (in the cell) not sorted at 1DPI	63	79	38	25	2.5	1.0
Manual injection (yolk center) not sorted at 1DPI	120	83	29	15	8.0	2.3
Full-automated (yolk center) selected using COPAS at 1DPI	524	35	52	15	34.9	5.2
Semi-automated injection (close to the cell) not sorted at 1DPI	223	25	43	20	11.2	4.1
Semi-automated injection (close to the cell) selected using COPAS at 1DPI	223	25	79	20	11.2	2.1

highly reproducible as estimated using plating of bacteria or CO-PAS analysis. We also have shown that COPAS analysis can reliably reproduce counting by bacterial plating thereby providing a versatile method for quantification of bacterial proliferation [97]. In addition to the capacity of the COPAS technology to sort embryos based on pre-set fluorescence or optical density properties, we show that it can also be useful for quantification of the distribution of injected particles using a specially designed Perl script. To demonstrate this we have analyzed the data obtained from a

M. marinum infection experiment in which the injected larvae were analyzed for bacterial spreading in the larva in the presence or absence of the antibiotic rifampicin. Zebrafish embryos between 16 and 64 cell stage were injected with 40 CFUs (colony forming units) of *M. marinum* strain E11 expressing the fluorescent protein mCherry. Three days post-injection larvae were analysed and pre-sorted using the COPAS XL (Union Biometrica). Pre-sorting settings were established in order to ensure a homogenous group of embryos presenting moderate infection levels, discarding

non-infected and highly infected embryos. Sorted larvae were treated with either 0.2% DMSO (control) or 200 μM rifampicin. Embryos were treated and infection levels were analyzed with COPAS XL for three days. The resulting optical density and red fluorescence profiles were analysed with a custom made script. The script reads the optical density and the red fluorescence profiles from a larva. It then divides both profiles in two and sums the optical density values and red fluorescence values for each half. The anterior half of the larvae is optically more dense compared to the posterior half and will have a higher sum. The lower optical density sum will determine the posterior half of the profile. The sum of the red fluorescence values for this half is the tail fluorescence and the sum of both halves is the total fluorescence. This allows us to analyse infection levels either in the whole larvae or in the tail section. The results (Fig. 1) show that bacteria can be detected with high sensitivity in the tail part of the larvae. We have also used this method for reanalysis of the previously published data set for *S. epidermidis* injection that was used for yielding a reference transcriptome database [97]. The results (Fig. 2) show that injected staphyloccoci massively spread into the tail part starting two days after injection providing quantitative data that further support the images from confocal laser scanning microscopy [97].

2.4. Injection of bacteria in combination with antisense morpholinos

The conventional procedure of gene function analysis during bacterial infection in zebrafish embryos is to inject morpholino oligonucleotides at 1–2 cell stage into yolk followed by bacterial injection into the caudal vein after the onset of blood circulation. This method is well-established but time consuming and low-throughput [81]. The labour intensity of such injections can be overcome by carrying out co-injection of morpholino and bacteria into the yolk of 1–2 cell stage zebrafish embryos using the automated injection system. This experimental setup was first tested using a morpholino oligonucleotide (GeneTools, Oregon, USA) designed against the transcription factor Pu-1 (Spi1) that blocks myeloid development [15]. These results confirmed the methodology and prompted us to investigate the function of more specific immune regulatory factors such as a follow up study on myeloid differentiation factor 88 (Myd88), an adaptor protein in Toll-like receptor signalling that has been studied by gene knock-down and gene knock-out analysis in zebrafish embryos, and shown to be involved in proinflammatory innate immune response to microbial infection [81,95]. For this, one nanoliter of myd88 morpholino at 1.6 mM concentration was co-injected with 40 CFUs of *M. marinum* at the 1–2 cell stage into the yolk of zebrafish embryo. Analysis of the fluorescence profile of 5 days post-injected embryos
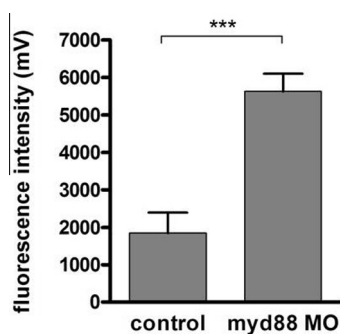
using the COPAS technology showed an increased bacterial burden in the morphant group compared to the control group due to knock-down of this gene (Fig. 3). These results mimic the already published infection studies with Myd88 knock-down, confirming that automatic yolk co-injection of morpholino and bacteria is capable of creating reproducible results for morpholino screens in a high-throughput manner.

2.5. Tumor cell implantation and screening for proliferation and spreading of cancer cells

2.5.1. Robotic injection of tumor cells

In manual injection experiments various tumor cell lines were shown to be highly different in their capacity to proliferate and spread into the entire zebrafish body after injection into the yolk of pre-gastrulation stage embryos. Pilot experiments using the injection robot with the highly aggressive osteosarcoma cell lines SJSA-1 (American Type Culture Collection , ATCC) and osteosarcoma line L2792 [13] showed a massive proliferation and strong spreading of fluorescent cells in the tail at 3 days post injection into the yolk at the 256-cell stage (Fig. 4). For further implantation assays shown in this paper, human prostate cells (PC3 and LNCap) and a highly angiogenic melanoma line (Mel57-VEGF) were used. The latter line was chosen because a stably transfected line was available that yielded a bright fluorescent signal that could be measured reproducibly at low cell counts using the COPAS technology.

In order to investigate the dissemination of tumor cells in zebrafish embryos, we developed an optimal setup for the establishment of a high-throughput xenograft model using the automated injection system. Cells were cultured as previously described i.e. in RPMI-1640 medium (Sigma Aldrich) supplemented with fetal bovine serum to a final concentration of 10%. Cells were subdivided 2–3 times a week at ratio of 1:5–1:10. Cultures were renewed every 8 passages. During subdividing care was taken that single cells were passed so no aggregates have formed. For transplantation, cells with 75–80% confluency should be used as they tend to clump less then more confluent cell cultures. For detection of
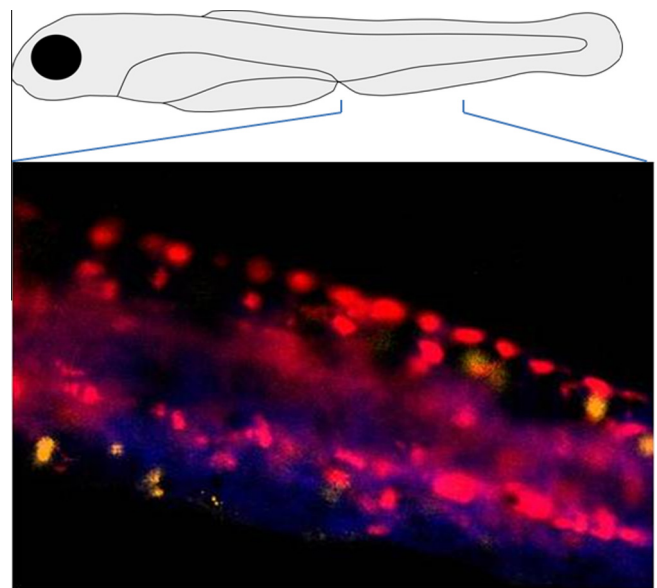

Fig. 3. Automatic co-injection of antisense morpholino and bacteria into yolk. Increased bacterial burden was measured using the COPAS system in myd88 and control morphants at 5 DPI following co-injection of *Mycobacterium marinum* with *myd88* morpholino into 1–2 cell stage zebrafish embryos. Asterisk indicate significant difference (***$p < 0.0001$) tested by unpaired *t*-test.

Fig. 4. Confocal laser scanning analysis of 5 days old larvae injected with osteosarcoma cell line SJSA-1 at the 256 cell stage. For these studies a transgenic zebrafish Tg (Fms:Gal4, UAS:mCherry) was used [36]. The figure shows a *z*-series projection of a part of the tail area with the mCherry signal shown in orange and the DiI of a multitude of cancer cells signal shown in red. Blue color represents autofluorescence.

cancer cells we mostly have used CM-DiI labeled cell cultures that were labeled using the following protocol: T75 flask with cells reaching 80% confluency were gently but quickly rinsed with 1 ml Trypsin–EDTA. For getting cells into suspension, cells were covered with 0.5 ml of Trypsin–EDTA and incubated for 2–5 min at 37 °C. Trypsination was stopped by adding 1 ml of PBS with 10% FCS and cell lumps were broken by gentle pipetting up and down. From this step no visible cell aggregates should be observed. Single cells were pelleted by centrifugation at 100g for 4 min in a 2 ml Eppendorf tube. Pellets were resuspended in 0.5 ml PBS with CM-DiI (InVitrogen) incubated first at 37 °C for 5 min and later at 4 °C for an additional quarter of an hour. After this step, cells were centrifuged again at 100g for 4 min, washed once in 0.5 ml PBS and counted. Finally cells were resuspended in 14% PVP to a final concentration of minimum 200 cells per microliter. Prior to injection, the labelled cells were kept at 34 °C and implanted within 3 h. Transgenic cells were treated in a similar way but the step related to incubation with a dye was omitted. As a control, fish were injected with 14% PVP. Due to the size of tumor cells, the suspension was loaded into glass capillary needles with bigger opening (Qvotech, 20 micron, Table 1). Up to 5 nl volume with minimum 400 cells were implanted using the robotic injector. Successfully injected embryos (around 80–90% rate) were either sorted manually under a fluorescence stereoscope (Leica) or sorted by the COPAS XL. Zebrafish embryos were maintained in groups of 50 in a Petridish with 20–25 ml egg water and kept at 34 °C until 6 DPI. Using a Tg (fli:GFP) endothelial reporter transgenic zebrafish line with fluorescent vasculature [49], we found that PC3 and LNCap cells transplanted robotically behaved in the same way as manually transplanted cells [34]. The first clearly disseminated fluorescent tumor cells were observed at 5 DPI in the caudal vein, and also in other small vascular in the eye and intersegmental vessels

(Fig. 5). These experiments showed several important technical aspects of the microinjection procedure. High concentration of PVP prevented cell clumping and needle clogging. However, as highly concentrated PVP is very viscous, it is difficult to work with. For cells that are kept in suspensions, lower concentration of PVP will be sufficient (e.g. 2%). It is also important to note that cell dissemination has only been observed when the number of implanted cells reached at least 400. When lower numbers of cells were implanted into an early embryo, even highly aggressive cells did not migrate out of the yolk.

2.5.2. Confocal screening and tumor cell dissemination

Taking advantage of the transparency of zebrafish larvae, we performed high-resolution confocal microscopy laser scanning imaging to characterize the dissemination of injected tumor cells in the case of the PC3 and LNCAP cell lines (500 cells injection). It is known that leukocytes contribute to different steps of tumor progression [39,77,82]. In order to investigate the role of embryonic myeloid cells in cancer cell spreading or killing of cancer cells, whole-mount L-plastin immunohistochemistry was carried out as described [56]. Antibodies and dilutions were used as follows: L-plastin rabbit anti-zebrafish primary antibody (provided by Dr. Huttenlocher), was diluted 1:500 and the secondary antibody (Alexa 568 anti-rabbit, Invitrogen) was used at a 1:200 dilution.

At 6 DPI, confocal imaging of fixed larvae revealed the presence of labeled cells in the vascular system, indicating that injected human tumor cells survived and disseminated outside the yolk (Fig. 6). Noteworthy, we also detected that labeled tumor cells were accompanied by a leukocyte population at various positions in the tissue (Fig. 6), suggesting that myeloid cells have a role in cancer cell recognition. In future studies we will study whether differences in dissemination are correlated with the aggressiveness of
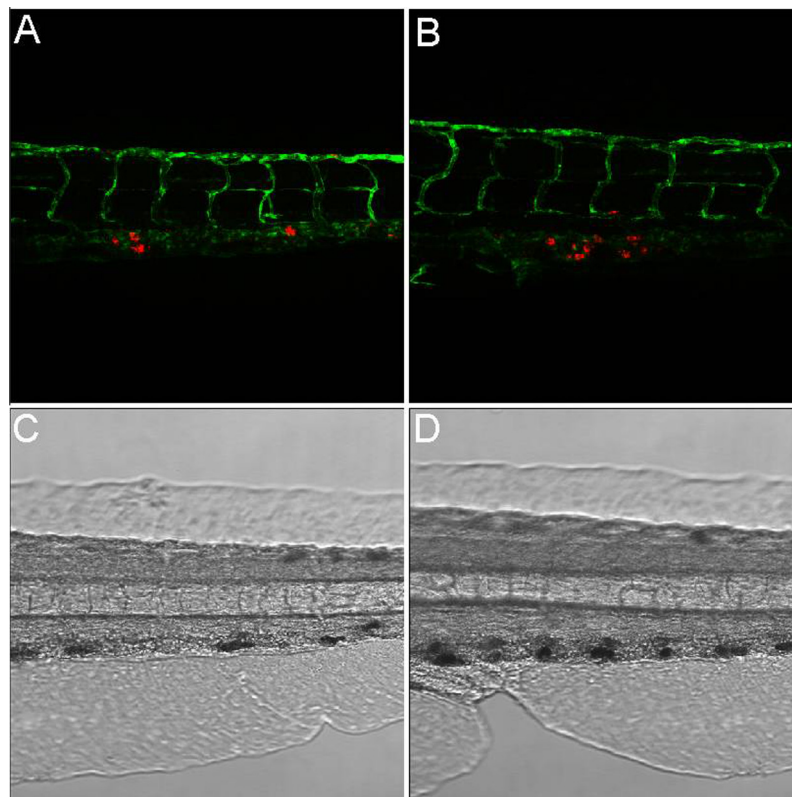

Fig. 5. Automatic injection of tumor cells into zebrafish embryos resulted in tumor dissemination. (A and B) confocal z-series projection and (C and D) bright-field of fluorescent cell tracker CM-DiI labeled LNCap cells disseminated to the tail vascular of a 7 day-old larva. Images were acquired using a Leica TCS SPE confocal microscope with a ×20 dry objective.
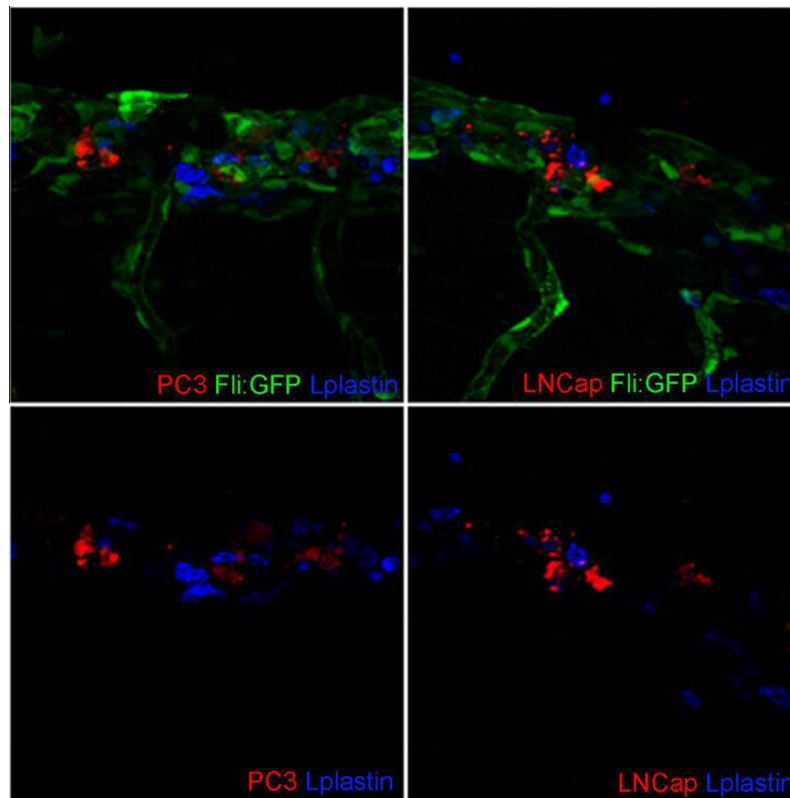
Fig. 6. Confocal screening of tumor cell dissemination in zebrafish embryos. PC3 and LNCaP (red color) injected in embryos showed clear dissemination from the original implantation site at 6 DPI. Leukocytes (in blue) associated with tumor cells are visible at the dissemination site with the vascular system in green (this signal is omitted in the in bottom panels). Two representative images are shown of embryonic leukocytes associated with fluorescent tumor cells at the caudal vein. Images were acquired using a Leica TCS SPE confocal microscope with a ×20 dry objective.

tumor cell type. For this we will use a combination of the automated injection system together with published high-throughput imaging technologies [34] to screen for the malignancy of many different mammalian cancer cell lines in the zebrafish embryo model at higher throughput levels than previously established.

2.5.3. COPAS screening for tumor cell proliferation

To demonstrate the survival rate and proliferation of injected tumor cells in zebrafish embryos, we employed a stably transfected melanoma cell line Mel57-VEGF expressing EGFP, [84] in our robotic injection system. A large set of embryos were injected with Mel57-EGFP cells (400 cell/embryo) at 2 and 4 hpf. The injected embryos were immediately run through the COPAS system to determine the total level of green fluorescence, which represents the injection load. The embryos were subsequently sorted with the following parameters: optical density threshold (extinction) = 390 mV (COPAS value: 20), minimum time of flight = 280 ms (COPAS value: 700), red photomultiplier tube (PMT) voltage = 0 V, green PMT voltage = 600 V, yellow PMT voltage = 0 V, fluorescent density threshold = 800. Successfully injected embryos were followed with the COPAS system until 6 DPI.

Combination of COPAS profiling and epifluorescence/brightfield imaging revealed significant tumor cell proliferation in the injected embryos (Fig. 7). At the first day after injection, the fluorescent signal of tumor clusters slightly dropped, suggesting a decrease of live cells due to the implantation process. At 6 DPI, the average signal per larva had significantly increased, and was almost 2-fold higher than than at 1 DPI (Fig. 7). These results illustrated the ability of COPAS to accurately quantify the number of tumor cells in zebrafish embryos. This shows that the combination of the automatic injection and COPAS sorting system provides a
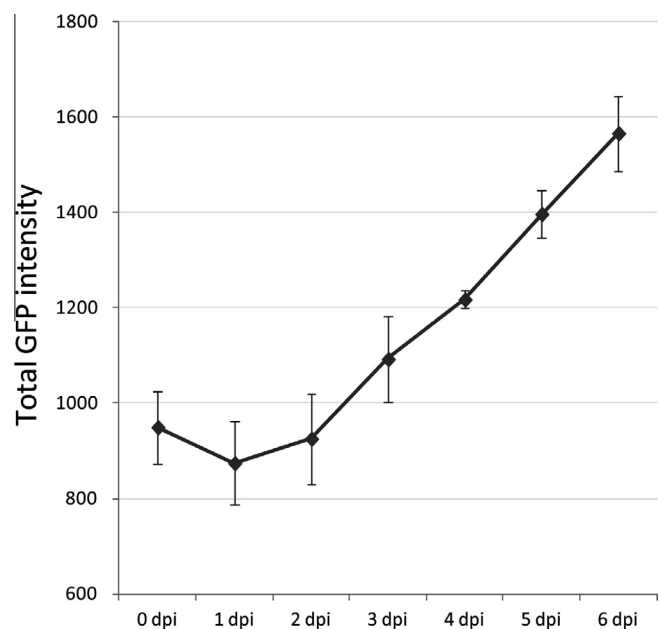

Fig. 7. Proliferation of automatic injected Mel57 cells in zebrafish embryos. Total fluorescent signal intensity quantifies the increase of tumor cell number in the injected embryos over 6 days. The sample size for each experiment was >400 embryos. More than 150 successfully injected embryos were sorted out at 1DPI. Final survival rate was >80% at 6DPI.

powerful in vivo platform for the investigation of human cancer proliferation, which in turn highly facilitates the discovery and screening of anti-cancer compounds directed at targets from the

Table 3
Overview of robotic injection applications. For details on the microbial robotic injection variables tested we also refer to Carvalho et al., 2011 [15] and Veneman et al., 2013 [97].

Robotic injection application	Variables tested	Limiting factors
DNA	• Position of injection • COPAS screening	• Higher accuracy of injection site will limit speed
Morpholinos	• Combination with microbial injection	• Morpholinos have to be injected as early as possible
Microbes	• Different types of microbes (e.g. Mycobacteria and Staphylococci) • Embryonic stage of injection • Microbial escape from yolk	• There is a delay period before bacteria from yolk will be exposed to cellular immune responses (e.g. phagocytosis) • For whole organism screening there will be background fluorescence from microbes in the yolk
Cancer cells	• Cancer cell types • PVP concentration • Spread to different body parts	• Embryo survival rates • Clumping of cells that will clog needles

implanted cells and the recipient host. Based on these results we have recently started with follow up studies using our methods of xenografting with many other cancer cell lines aimed at obtaining mechanistic insights in the spreading of cancer cells through the zebrafish body. These studies already have indicated that using this methodology new knowledge can be obtained in proliferation and metastatic behaviour of Ewing's sarcoma cells (manuscript in preparation). This is of clinical relevance since at the time of diagnosis ~25% of Ewing's sarcoma patients, predominantly children and young adults, present with metastatic disease and a poor survival prognosis. In case of recurrence of the disease, overall survival rates are as low as ~10–20%. Although the causative underlying defect is known, there are currently no reliable treatment strategies for this malignant bone tumor. Therefore, high-throughput screening is greatly needed for rapid pre-clinical drug screens for this type of tumor.

3. Conclusions

The provided methods for robotic microinjection of DNA, morpholinos, bacteria and cancer cells in zebrafish embryos enables the generation of an abundance of reproducibly treated living test models. In Table 3 we present a summary of variables that we have tested with our developed technology. We have shown that this technology benefits optimally from many new high-throughput screening methods. These methods are not only applicable to the disease models highlighted in this paper, i.e. cancer and infectious disease, but are widely applicable to studies that benefit from the use of small transparent zebrafish larvae. We anticipate that our technology is also applicable to other fish models. For instance the use of carp fish, which are easy to culture and have a clutch size of hundred thousands of eggs in one spawn, would be extremely useful for screens in larvae at ultra high-throughput level [1]. We have recently generated a draft genome of the European common carp (Cyprinus carpio carpio) showing a striking gene similarity with the zebrafish, but, a much higher compactness of the genome, making it highly interesting for further comparative studies with zebrafish at the genetic level [41]. In our own research we will continue to use zebrafish and other fish species for applications in disease studies, but, we will also give more attention to the applicability of our methodology for toxicology research in zebrafish [30]. This is because we believe that the combination of screens for potential new therapeutics will benefit greatly in speed by a combination with toxicology approaches. In the near future the use of our microinjection technology will also be used for detailed drug RP/KD studies that should give indications on the translatability of drug treatment effects and might suggest protocols for optimized drug administration. For this the injection of synthetic slow or controlled release vehicles in combination with highly sensitive detection of compounds using mass spectrometry will be highly valuable [69–71,76].

References

[1] S. Ali, D.L. Champagne, H.P. Spaink, M.K. Richardson, Birth Defects Res. C Embryo Today 93 (2011) 115–133.
[2] J.P. Allen, M.N. Neely, Future Microbiol. 5 (2010) 563–569.
[3] J.F. Amatruda, E.E. Patton, Int. Rev. Cell Mol. Biol. 271 (2008) 1–34.
[4] K.V. Anderson, P.W. Ingham, Nat. Genet. 33 (Suppl.) (2003) 285–293.
[5] J. Bakkers, Cardiovasc. Res. 91 (2011) 279–288.
[6] V.M. Bedell, Y. Wang, J.M. Campbell, T.L. Poshusta, C.G. Starker, R.G. Krug, W. Tan, S.G. Penheiter, A.C. Ma, A.Y. Leung, S.C. Fahrenkrug, D.F. Carlson, D.F. Voytas, K.J. Clark, J.J. Essner, S.C. Ekker, Nature 491 (2012) 114–118.
[7] E.L. Benard, A.M. van der Sar, F. Ellett, G.J. Lieschke, H.P. Spaink, A.H. Meijer, J. Vis. Exp. 61 (2012).
[8] R.D. Berg, L. Ramakrishnan, Trends Mol. Med. 18 (2012) 689–690.
[9] J. Berger, P.D. Currie, Dis. Model. Mech. 5 (2012) 726–732.
[10] B.R. Bill, A.M. Petzold, K.J. Clark, L.A. Schimmenti, S.C. Ekker, Zebrafish 6 (2009) 69–77.
[11] J.P. Briggs, Am. J. Physiol. Regul. Integr. Comp. Physiol. 282 (2002) R3–R9.
[12] K.M. Brothers, R.T. Wheeler, J. Vis. Exp. 65 (2012).
[13] E.P. Buddingh, M.W. Schilham, S.E. Ruslan, D. Berghuis, K. Szuhai, J. Suurmond, A.H. Taminiau, H. Gelderblom, R.M. Egeler, M. Serra, P.C. Hogendoorn, A.C. Lankester, Cancer Immunol. Immunother. 60 (2011) 575–586.
[14] L. Cade, D. Reyon, W.Y. Hwang, S.Q. Tsai, S. Patel, C. Khayter, J.K. Joung, J.D. Sander, R.T. Peterson, J.R. Yeh, Nucleic Acids Res. 40 (2012) 8001–8010.
[15] R.P. Carvalho, J. de Sonneville, O.W. Stockhammer, N.D.L. Savage, W.J. Veneman, T.H.M. Ottenhoff, R.P. Dirks, A.H. Meijer, H.P. Spaink, PLoS One 6 (2011) e16779.
[16] T.Y. Chang, C. Pardo-Martin, A. Allalou, C. Wahlby, M.F. Yanik, Lab Chip 12 (2012) 711–716.
[17] S. Chatterjee, T. Lufkin, Curr. Top. Genet. 5 (2012) 1–10.
[18] E. Chen, S.C. Ekker, Curr. Pharm. Biotechnol. 5 (2004) 409–413.
[19] K. Chen, R.B. Cole, B.B. Rees, J. Proteomics 78 (2013) 477–485.
[20] S. Chen, G. Oikonomou, C.N. Chiu, B.J. Niles, J. Liu, D.A. Lee, I. Antoshechkin, D.A. Prober, Nucleic Acids Res. 41 (2013) 2769–2778.

[21] K.J. Clark, D.F. Voytas, S.C. Ekker, Zebrafish 8 (2011) 147–149.
[22] D.P. Corkery, G. Dellaire, J.N. Berman, Br. J. Haematol. 153 (2011) 786–789.
[23] M.J. Crim, L.K. Riley, ILAR J. 53 (2012) 135–143.
[24] C. Cui, E.L. Benard, Z. Kanwal, O.W. Stockhammer, M. van der Vaart, A. Zakrzewska, H.P. Spaink, A.H. Meijer, Methods Cell Biol. 105 (2011) 273–308.
[25] T.J. Dahlem, K. Hoshijima, M.J. Jurynec, D. Gunther, C.G. Starker, A.S. Locke, A.M. Weis, D.F. Voytas, D.J. Grunwald, PLoS Genet. 8 (2012) e1002861.
[26] Detrich, Essential Zebrafish Methods: Cell and Developmental Biology, Academic Press, Oxford, 2009.
[27] Detrich, The Zebrafish: Disease Models and Chemical Screens, Elsevier, Amsterdam, 2011.
[28] Detrich, The Zebrafish: Genetics, Genomics and Informatics, Elsevier, Amsterdam, 2011.
[29] M.C. Dovey, L.I. Zon, Methods Mol. Biol. 568 (2009) 1–5.
[30] M. Driessen, A.S. Kienhuis, J.L. Pennings, T.E. Pronk, E.J. van de Brandhof, M. Roodbergen, H.P. Spaink, B. van de Water, L.T. van der Ven, Arch. Toxicol. 87 (2013) 807–823.
[31] J. Etchin, J.P. Kanki, A.T. Look, Methods Cell Biol. 105 (2011) 309–337.
[32] Y. Feng, C. Santoriello, M. Mione, A. Hurlstone, P. Martin, PLoS Biol. 8 (2010) e1000562.
[33] J. Gehrig, M. Reischl, E. Kalmar, M. Ferg, Y. Hadzhiev, A. Zaucker, C. Song, S. Schindler, U. Liebel, F. Muller, Nat. Methods 6 (2009) 911–916.
[34] V.P. Ghotra, S. He, B.H. de, W. van der Ent, H.P. Spaink, B. van de Water, B.E. Snaar-Jagalska, E.H. Danen, PLoS One 7 (2012) e31281.
[35] W. Goessling, T.E. North, L.I. Zon, J. Clin. Oncol. 25 (2007) 2473–2479.
[36] C. Gray, C.A. Loynes, M.K. Whyte, D.C. Crossman, S.A. Renshaw, T.J. Chico, Thromb. Haemost. 105 (2011) 811–819.
[37] D.J. Grunwald, J.S. Eisen, Nat. Rev. Genet. 3 (2002) 717–724.
[38] M. Haldi, C. Ton, W.L. Seng, P. McGrath, Angiogenesis 9 (2006) 139–151.
[39] S. He, G.E. Lamers, J.W. Beenakker, C. Cui, V.P. Ghotra, E.H. Danen, A.H. Meijer, H.P. Spaink, B.E. Snaar-Jagalska, J. Pathol. 227 (2012) 431–445.
[40] Z. Hegedus, A. Zakrzewska, V.C. Agoston, A. Ordas, P. Racz, M. Mink, H.P. Spaink, A.H. Meijer, Mol. Immunol. 46 (2009) 2918–2930.
[41] C.V. Henkel, R.P. Dirks, H.J. Jansen, M. Forlenza, G.F. Wiegertjes, K. Howe, G.E. van den Thillart, H.P. Spaink, Zebrafish 9 (2012) 59–67.
[42] S. Hogl, B.F. van, B. Dislich, P.H. Kuhn, C. Haass, B. Schmid, S.F. Lichtenthaler, Proteomics 13 (2013) 1519–1527.
[43] P. Huang, Z. Zhu, S. Lin, B. Zhang, J. Genet. Genomics 39 (2012) 421–433.
[44] L. Jing, L.I. Zon, Dis. Model. Mech. 4 (2011) 433–438.
[45] S. Kabli, H.P. Spaink, H.J. De Groot, A. Alia, J. Magn. Reson. Imaging 29 (2009) 275–281.
[46] M. Kanther, J.F. Rawls, Curr. Opin. Immunol. 22 (2010) 10–19.
[47] D. Kokel, J. Bryan, C. Laggner, R. White, C.Y. Cheung, R. Mateus, D. Healey, S. Kim, A.A. Werdich, S.J. Haggarty, C.A. Macrae, B. Shoichet, R.T. Peterson, Nat. Chem. Biol. 6 (2010) 231–237.
[48] M. Konantz, T.B. Balci, U.F. Hartwig, G. Dellaire, M.C. Andre, J.N. Berman, C. Lengerke, Ann. N. Y. Acad. Sci. 1266 (2012) 124–137.
[49] N.D. Lawson, B.M. Weinstein, Dev. Biol. 248 (2002) 307–318.
[50] L.M. Lee, E.A. Seftor, G. Bonde, R.A. Cornell, M.J. Hendrix, Dev. Dyn. 233 (2005) 1560–1570.
[51] Lieschke, Zebrafish: Methods and Protocols, Springer protocols, Heidelberg, 2008.
[52] G.J. Lieschke, P.D. Currie, Nat. Rev. Genet. 8 (2007) 353–367.
[53] C. Lossner, S. Wee, S.G. Ler, R.H. Li, T. Carney, W. Blackstock, J. Gunaratne, Proteomics 12 (2012) 1879–1882.
[54] M.B. Lucitt, T.S. Price, A. Pizarro, W. Wu, A.K. Yocum, C. Seiler, M.A. Pack, I.A. Blair, G.A. Fitzgerald, T. Grosser, Mol. Cell. Proteomics 7 (2008) 981–994.
[55] J.S. Martin, S.A. Renshaw, Biochem. Soc. Trans. 37 (2009) 830–837.
[56] J.R. Mathias, M.E. Dodd, K.B. Walters, J. Rhodes, J.P. Kanki, A.T. Look, A. Huttenlocher, J. Cell Sci. 120 (2007) 3372–3383.
[57] A.H. Meijer, H.P. Spaink, Curr. Drug Targets 12 (2011) 1000–1017.
[58] K. Milligan-Myhre, J.R. Charette, R.T. Phennicie, W.Z. Stephens, J.F. Rawls, K. Guillemin, C.H. Kim, Methods Cell Biol. 105 (2011) 87–116.
[59] M. Mione, A.H. Meijer, B.E. Snaar-Jagalska, H.P. Spaink, N.S. Trede, Zebrafish 6 (2009) (2009) 445–451.
[60] M. Mione, L.I. Zon, Curr. Biol. 22 (2012) R522–R525.
[61] M.C. Mione, N.S. Trede, Dis. Model. Mech. 3 (2010) 517–523.
[62] I. Mizgirev, S. Revskoy, Nat. Protoc. 5 (2010) 383–394.
[63] A.B. Mohseny, W. Xiao, R. Carvalho, H.P. Spaink, P.C. Hogendoorn, A.M. Cleton-Jansen, J. Pathol. 227 (2012) 245–253.
[64] F.E. Moore, D. Reyon, J.D. Sander, S.A. Martinez, J.S. Blackburn, C. Khayter, C.L. Ramirez, J.K. Joung, D.M. Langenau, PLoS One 7 (2012) e37877.
[65] B. Novoa, A. Figueras, Adv. Exp. Med. Biol. 946 (2012) 253–275.
[66] A. Ordas, Z. Hegedus, C.V. Henkel, O.W. Stockhammer, D. Butler, H.J. Jansen, P. Racz, M. Mink, H.P. Spaink, A.H. Meijer, Fish Shellfish Immunol. 31 (2010) 716–724.
[67] C. Pardo-Martin, T.Y. Chang, B.K. Koo, C.L. Gilleland, S.C. Wasserman, M.F. Yanik, Nat. Methods 7 (2010) 634–636.
[68] E. Payne, T. Look, Br. J. Haematol. 146 (2009) 247–256.
[69] K. Peng, C. Cui, I. Tomatsu, F. Porta, A.H. Meijer, H.P. Spaink, A. Kros, Soft Matter 6 (2010) 13778–13783.
[70] K. Peng, I. Tomatsu, B. van den Broek, C. Cui, A.V. Korobko, J. van Noort, A.H. Meijer, H.P. Spaink, A. Kros, Soft Matter 7 (2011) 4881–4887.
[71] R.J. Raterink, F.M. Kloet, J. Li, N.A. Wattel, M.J.M. Schaaf, H.P. Spaink, R. Berger, R.J. Vreeken, T. Hankemeier, Metabolomics (2013) 1–10.
[72] S.A. Renshaw, P.W. Ingham, BMC Biol. 8 (2010) 148.
[73] S.A. Renshaw, N.S. Trede, Dis. Model. Mech. 5 (2012) 38–47.
[74] J. Richardson, Z. Zeng, C. Ceol, M. Mione, I.J. Jackson, E.E. Patton, Pigm. Cell Melanoma Res. 24 (2011) 378–381.
[75] S. Santana, E.P. Rico, J.S. Burgos, Am. J. Neurodegener. Dis. 1 (2012) 32–48.
[76] F. Sharif, F. Porta, A.H. Meijer, A. Kros, M.K. Richardson, Int. J. Nanomedicine 7 (2012) 1875–1890.
[77] F. Shojaei, N. Ferrara, Cancer Res. 68 (2008) 5501–5504.
[78] J.M. Spitsbergen, M.L. Kent, Toxicol. Pathol. 31 (Suppl) (2003) 62–87.
[79] J. Sprague, L. Bayraktaroglu, D. Clements, T. Conlin, D. Fashena, K. Frazer, M. Haendel, D.G. Howe, P. Mani, S. Ramachandran, K. Schaper, E. Segerdell, P. Song, B. Sprunger, S. Taylor, C.E. Van Slyke, M. Westerfield, Nucleic Acids Res. 34 (2006) D581–D585.
[80] H.M. Stern, L.I. Zon, Nat. Rev. Cancer 3 (2003) 533–539.
[81] O.W. Stockhammer, A. Zakrzewska, Z. Hegedus, H.P. Spaink, A.H. Meijer, J. Immunol. 182 (2009) 5641–5653.
[82] C. Stockmann, A. Doedens, A. Weidemann, N. Zhang, N. Takeda, J.I. Greenberg, D.A. Cheresh, R.S. Johnson, Nature 456 (2008) 814–818.
[83] K. Stoletov, R. Klemke, Oncogene 27 (2008) 4509–4520.
[84] T.H. Stollman, M.G. Scheer, G.M. Franssen, K.N. Verrijp, W.J. Oyen, T.J. Ruers, W.P. Leenders, O.C. Boerman, Cancer Biother. Radiopharm. 24 (2009) 195–200.
[85] U. Strahle, S. Scholz, R. Geisler, P. Greiner, H. Hollert, S. Rastegar, A. Schumacher, I. Selderslaghs, C. Weiss, H. Witters, T. Braunbeck, Reprod. Toxicol. 33 (2012) 128–132.
[86] K. Takaki, C.L. Cosma, M.A. Troll, L. Ramakrishnan, Cell Rep. 2 (2012) 175–184.
[87] A.M. Taylor, L.I. Zon, Zebrafish 6 (2009) 339–346.
[88] K.L. Taylor, N.J. Grant, N.D. Temperley, E.E. Patton, Cell Commun. Signal. 8 (2010) 11.
[89] J. Terriente, C. Pujades, Dev. Dyn. 242 (2013) 97–107.
[90] C. Tobia, G. Gariano, S.G. De, M. Presta, Biochim. Biophys. Acta 1832 (2013) 1371–1377.
[91] D.M. Tobin, R.C. May, R.T. Wheeler, PLoS Pathog. 8 (2012) e1002349.
[92] D.M. Tobin, L. Ramakrishnan, Cell. Microbiol. 10 (2008) 1027–1039.
[93] N.S. Trede, W. Heaton, S. Ridges, H. Sofla, M. Cusick, D. Bearss, D. Jones, R.S. Fujinami, Curr. Protoc. Pharmacol. 60 (2013) 14.24.1–14.24.13. Chapter 14, Unit14.
[94] M. van der Vaart, H.P. Spaink, A.H. Meijer, Adv. Hematol. 2012 (2012) 159807.
[95] M. van der Vaart, J.J. van Soest, H.P. Spaink, A.H. Meijer, Dis. Model. Mech. (2013), http://dx.doi.org/10.1242/dmm.010843.
[96] J.J. van Soest, O.W. Stockhammer, A. Ordas, G.V. Bloemberg, H.P. Spaink, A.H. Meijer, BMC Immunol. 12 (2011) 58.
[97] W.J. Veneman, O.W. Stockhammer, B.L. de, S.A. Zaat, A.H. Meijer, H.P. Spaink, BMC Genomics 14 (2013) 255.
[98] W. Wang, X. Liu, D. Gelinas, B. Ciruna, Y. Sun, PLoS One 2 (2007) e862.
[99] M. Westerfield, The Zebrafish Book: A Guide for the Laboratory Use of Zebrafish Danio (Brachydanio) rerio, Univ. of Oregon Press, Eugene, 2000.
[100] R.M. White, J. Cech, S. Ratanasirintrawoot, C.Y. Lin, P.B. Rahl, C.J. Burke, E. Langdon, M.L. Tomlinson, J. Mosher, C. Kaufman, F. Chen, H.K. Long, M. Kramer, S. Datta, D. Neuberg, S. Granter, R.A. Young, S. Morrison, G.N. Wheeler, L.I. Zon, Nature 471 (2011) 518–522.